Zonal flow and field generation by finite beta drift waves and kinetic drift-Alfvén waves

P. N. Guzdar[a] and R. G. Kleva
Institute for Research in Electronics and Applied Physics, University of Maryland, College Park, Maryland 20742-3511

A. Das and P. K. Kaw
Institute for Plasma Research, Bhat, Gandhinagar, Gujarat

(Received 12 December 2000; accepted 29 May 2001)

A study of the generation of zonal flows and zonal magnetic fields by finite beta drift waves and kinetic drift-Alfvén waves is presented. The analysis is a generalization of recent investigations of the modulational instability for zonal flow generation by electrostatic drift waves to finite beta drift waves and kinetic drift-Alfvén waves. The drift wave driven unstable zonal flows/fields are stabilized by finite β below a critical value, due to the finite beta modification of the drift wave pump and the drift sidebands. They are, however, destabilized by coupling to the zonal field for larger β. The drift-Alfvén branch driven zonal flows/fields are found to be completely stable below a critical β, and are destabilized for larger β. These new results can find applications in a variety of laboratory and space plasma situations.
[DOI: 10.1063/1.1386640]

I. INTRODUCTION

The existence of shear flows in fluids and plasmas is a ubiquitious phenomenon. In tokamak plasmas shear flow plays a fundamental role in the various improved confinement states observed over the years. The observation of the low to high confinement (L–H) transition in tokamaks heralded significant optimism for achieving the goal of fusion in a laboratory plasma.[1–3] More recently, the enhanced confined modes observed in all the major devices has also has added to the optimism.[4,5] In space plasmas, shear flow[6,7] is observed in the high latitude ionosphere and has been used successfully in driving a variety of instabilities to explain the rich spectrum of electrostatic and electromagnetic instabilites observed by satellites. By assuming the existence of shear flow, Ganguli *et al.*,[8] have identified a hierarchy of waves, from high frequency waves near the lower hybrid frequency and scale-lengths between the electron and ion gyro-radii, to cyclotron waves (the inhomogeneous energy density driven instability) with scale lengths of the order but larger than the ion gyro-radius, to low frequency Kelvin–Helmholtz modes with frequency below the ion gyro-frequency and scale-lengths much longer than the ion gyro-radius, which can be driven unstable by velocity shear perpendicular to the magnetic field. In laboratory table-top experiments[9–12] the interaction of self-consistently generated shear flow and driven vortices have provided great insight into the generation mechanisms. These are but a few examples of the pervasiveness of shear flows in nature and in laboratory experiments. Thus understanding the generation of shear flow has been actively pursued.

The linear instability for investigating the generation of shear flow in fluids and plasmas involves assuming the existence of a large amplitude wave pump with a given mode number and frequency (in the case of plasmas) and studying the stability of this wave to the shear flow and the nearest side bands, which couple the shear flow to the pump. For the case of fluids, the large amplitude wave may be some driven vortices in incompressible fluids or Rossby waves in geostrophic fluids. In the case of plasmas these may be natural modes like, for instance, the drift wave [and its various incarnations like the ion temperature gradient (ITG) mode and electron temperature (ETG) gradient mode]. We have recently reviewed the study of shear flow generation in fluids and plasmas with a focus on the linear instability analysis[13] and, therefore, will refer the reader to this article for details. Basically the various studies can be classified into two categories. The first one uses the classical coherent parametric instability approach to study the mechanism associated with the generation of shear flow.[13–20] In the second approach,[21–26] the drift waves are represented by a wave-kinetic equation coupled to the zonal flow equation. In the wave-kinetic analysis there is an intrinsic separation in the scale-lengths between the "short" scale drift wave and the long scale zonal flows. Both these studies obtain conditions for the growth for the "modulational" instability for the generation of shear flow, though their scalings and regimes of validity are different. Once again we direct the interested reader to our earlier work.[13] Our goal in the present work is to report on results of shear flow generation in finite beta plasmas using the coherent modulational instability analysis. Gruzinov *et al.*[27] have used the wave-kinetic approach to study the dynamo problem. Our modulational instability analysis allows for additional natural modes like the shear Alfvén modes to generate flows and it also addresses the role of finite beta effects on the generation of shear flows by electrostatic drift waves (including ITG and ETG modes). We believe that our findings will have implications in a va-

[a]Electronic mail: guzdar@glue.umd.edu

riety of applications. Recently we have applied some of these results to explaining low–high (L–H) transitions in tokamaks.[28]

II. BASIC EQUATIONS

The basic equations that are used have been derived by Zeiler *et al.*[29] They are

$$\frac{dn}{dt}+\frac{c_s^2}{\Omega_i}\frac{1}{L_n}\frac{\partial\phi}{\partial y}-\nabla_\parallel J=0, \tag{1}$$

$$\frac{c_s^2}{\Omega_i^2}\nabla_\perp\frac{d}{dt}\nabla_\perp\phi-\nabla_\parallel J=0, \tag{2}$$

$$\frac{\partial\psi}{\partial t}+\frac{c_s^2}{\Omega_i}\frac{1}{L_n}\frac{\partial\psi}{\partial y}-v_A\nabla_\parallel(\phi-n)=0, \tag{3}$$

with

$$J=v_A\frac{c_s^2}{\Omega_i^2}\nabla_\perp^2\psi, \tag{4}$$

$$\nabla_\parallel=\nabla_{\parallel 0}+\frac{c_s^2R_0}{\Omega_i v_A}\nabla\zeta\times\nabla\psi\cdot\nabla, \tag{5}$$

and

$$\frac{d}{dt}=\frac{\partial}{\partial t}+\frac{c_s^2R_0}{\Omega_i}\nabla\zeta\times\nabla\phi\cdot\nabla. \tag{6}$$

Here $n=\tilde{n}/n_0$, $\phi=e\tilde{\phi}/T_e$, $\psi=(\Omega_i v_A/c_s^2B_0)\tilde{\psi}$ are the normalized perturbed density, electrostatic potential, and parallel vector potential, respectively. In these equations R_0 is the major radius, Ω_i is the ion gyro-radius, c_s the ion acoustic speed computed with only the electron temperature, L_n is the density gradient scale length, v_A is the Alfvén velocity, and ζ is the toroidal angle. Here a few comments are in order. We have neglected the curvature terms as well as any dissipation effects. Our goal is to provide as simple a derivation of the instability as possible.

III. ZONAL FLOW-FIELD INSTABILITY

We first develop a low-dimensional model for the generation of shear/zonal flow and magnetic field by assuming that all the three quantities n, ϕ, and ψ for the pump wave can be written as

$$\xi=\xi_0\exp(ik_yy+ik_\parallel z-i\omega_0t), \tag{7}$$

where ξ represents any one of the three quantities.

Now for the perturbed quantites which couple the pump wave with zonal and field flows, the two potentials ϕ and ψ can be represented as

$$\begin{aligned}\xi=&\xi_s\exp(ik_xx-i\omega t)+\xi_+\exp(+ik_xx+ik_yy+ik_\parallel z-i\omega_+t)\\&+\xi_-\exp(ik_xx-ik_yy-ik_\parallel z-i\omega_-t),\end{aligned} \tag{8}$$

where $\omega_\pm=\omega\pm\omega_0$. The density perturbations do not have any purely k_x component, but have the two sidebands n_+ and n_-. This representation is the local version of that used by Chen *et al.*,[20] and the complex representation of that used by Guzdar.[13,19] The four coupled equations for zonal, field flows and the sidebands are

$$(\omega+\Delta)\phi_+=i\Gamma[M_A\phi_0\phi_s+M_B\phi_0\psi_s], \tag{9}$$

$$(\omega-\Delta)\phi_-=-i\Gamma[M_A\phi_0^*\phi_s+M_B\phi_0^*\psi_s], \tag{10}$$

$$(\omega+i\nu)\phi_s=i\Gamma\left[1-\left(\frac{\omega_0}{k_\parallel v_A}\right)^2\right][\phi_0^*\phi_+-\phi_0\phi_-], \tag{11}$$

$$(\omega+i\nu_M)\psi_s=i\Gamma\left(\frac{\omega_0}{k_\parallel v_A}\right)^2[\phi_0^*\phi_+-\phi_0\phi_-]. \tag{12}$$

Here

$$\begin{aligned}M_A=&\left[1-2\frac{\omega_0}{k_\parallel^2v_A^2}\left(\omega_0-\frac{\omega_*}{2}\right)\right.\\&\left.+\frac{k_x^2-k_y^2}{k_\perp^2}\left(1-\frac{\omega_*}{\omega_0}-k_x^2\rho_s^2\right)\right]\Big/A,\end{aligned} \tag{13}$$

$$M_B=-\left[\frac{2k_y^2}{k_\perp^2}\left(1-\frac{\omega_*}{\omega_0}+k_y^2\rho_s^2\right)\right]\Big/A, \tag{14}$$

$$A=1+k_\perp^2\rho_s^2-\frac{3\omega_0(\omega_0-2\omega_*/3)}{k_\parallel^2v_A^2}. \tag{15}$$

The parameter $\Delta=k_x^2\rho_s^2\omega_0/A$ is the frequency shift between the pump wave and the sidebands. This frequency shift arises due to the dispersive nature of the drift and kinetic drift-Alfvén waves. Here $k_\perp^2=k_x^2+k_y^2$, $\omega_*=k_y\rho_sc_s/L_n$ is the electron diamagnetic frequency and $\gamma_s=\Gamma|\phi_0|=(k_xk_yc_s^2/\Omega_i)|\phi_0|$ is the maximum growth rate for the shear flow instability for the electrostatic case.

The drift wave and drift-Alfvén wave pumps satisfy the dispersion relation

$$1+k_y^2\rho_s^2-\frac{\omega_*}{\omega_0}-\frac{\omega_0(\omega_0-\omega_*)}{k_\parallel^2v_A^2}=0. \tag{16}$$

The general dispersion relation obtained from this system of equations is

$$\begin{aligned}(\omega+i\nu)(\omega+i\nu_M)=&-\frac{2\omega\gamma_s^2}{\omega^2-\Delta^2}\left\{(\omega+i\nu_M)M_A\right.\\&\times\left[1-\left(\frac{\omega_0}{k_\parallel v_A}\right)^2\right]\\&\left.+(\omega+i\nu)M_B\left(\frac{\omega_0}{k_\parallel v_A}\right)^2\right\}.\end{aligned} \tag{17}$$

This dispersion relation is the finite-beta slab version of Eq. (10) in the work of Chen *et al.*[12] and also includes the large mode-number limit because of the terms associated with the nonlinear polarization drift in the drift-wave components. In the limit of $v_A\to\infty$, the dispersion relation reduces to that for the electrostatic case derived in Guzdar *et al.*,[6]

$$(\omega+i\nu)+\frac{2\omega\gamma_s^2}{\omega^2-\Delta^2}(1+k_y^2\rho_s^2-k_x^2\rho_s^2)=0. \tag{18}$$

If we examine the finite beta dispersion relation [Eq. (17)], we find that there are two distinct finite β effects. The first such effect, which appears in the matrix element M_A is due to the finite β associated with the pump wave, which in this case can be either the drift branch or the two kinetic shear Alfvén branches. The second finite beta effect arises because of the zonal field ψ_s. The nature of the coupling shows that the zonal flow and the zonal field are on the same footing, both being driven by the pump wave and the two sidebands. For the more general case we solve the equations numerically. We further simplify the problem by assuming that the damping coefficients $\nu=\nu_M=0$. The damping for the zonal flow in the slab geometry arises from the ion–ion collisions. This is indeed very small compared to the growth rates for even modest levels of the amplitude of the pump. The damping of the zonal field, on the other hand, is due to the electron plasma resistivity. It becomes important for very short scale-lengths compared to the collisional skin depth. Again here we can assume that the scale-length of interest is in the range of the ion gyro-radius with electron temperature, which is larger than the collisional skin depth, so that we can neglect the damping of the zonal field.

IV. NUMERICAL RESULTS

To solve the dispersion relation [Eq. (17)], it is first necessary to solve dispersion relation for the pump drift and drift Alfvén waves [Eq. (16)]. Normalizing the frequency ω_0 to the drift frequency ω_*, and assuming $k_\parallel \sim (qR)^{-1}$, the normalized dispersion relation [Eq. (16)] becomes

$$1+k_y^2\rho_s^2-\frac{1}{\Omega_0}-\Omega_0 k_y^2\rho_s^2\hat{\beta}(\Omega_0-1)=0, \tag{19}$$

subsequently the growth rate for the shear/zonal flow and field [Eq. (17)] becomes

$$\gamma=(k_x\rho_s)(k_y\rho_s)[M_A(1-\Omega_0^2k_y^2\rho_s^2\hat{\beta}) + M_B\Omega_0^2k_x^2\rho_s^2k_y^2\rho_s^2\hat{\beta}-\hat{\Delta}^2]^{1/2}. \tag{20}$$

Here $\Omega_0=\omega_0/\omega_*$, $\hat{\beta}=\beta(qR/L_n)^2/2$ with $\beta=8\pi nT_e/B^2$ and $\hat{\Delta}^2=(1/2)(\rho_s/L_n)^2(k_x\rho_s)^2\Omega_0^2/|\phi_0|^2$. Also the growth rate has been normalized to $\Omega_i|\phi_0|$. These normalizations show that there are four dimensionless parameters, (1) $k_y\rho_s$, (2) $k_x\rho_s$, (3) $\hat{\beta}$, and (4) $|\phi_0|L_n/\rho_s$. In these studies we will assume that $|\phi_0|=\rho_s/L_n$. We investigate the role of the three other dimensionless parameters. The simple dispersion relation [Eq. (20)] for the growth rate yields very interesting results for the generation of shear/zonal flow and field.

Shown in Figs. 1(a) and 1(b) are the dispersion curves for the drift wave and drift-Alfvén branches respectively for $k_y\rho_s=0.25$ (solid line) and $k_y\rho_s=0.50$ (dashed line) as a function of β. As seen from the plots, the inclusion of finite beta strongly reduces the frequency of the drift wave as well as the drift-Alfvén branch (in these normalized units). Using these eigenfrequencies, we now compute the growth rate for the shear/zonal flow and field. In Figs. 2(a) and 2(b), the

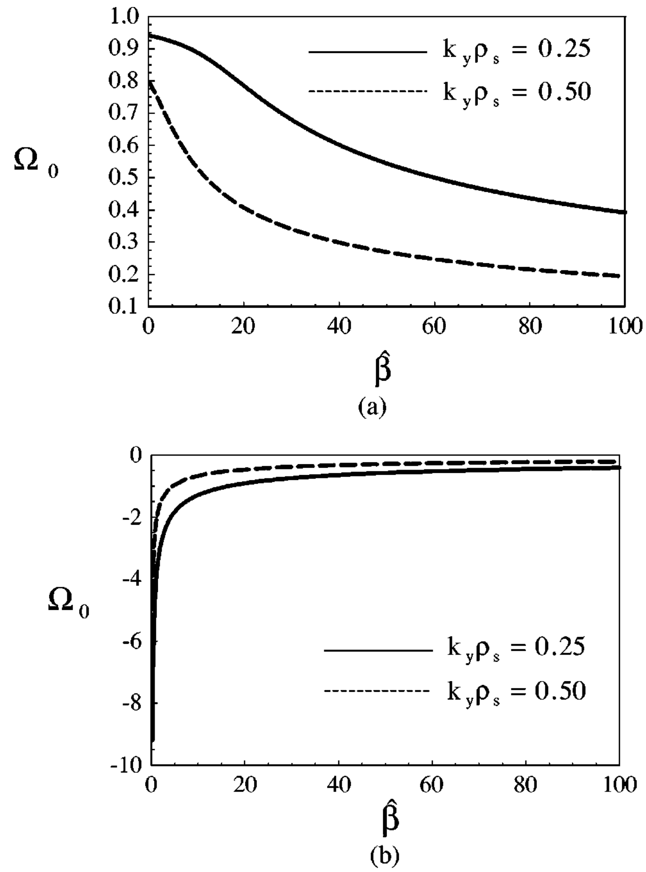

FIG. 1. (a) Eigenfrequency Ω_0 for drift-wave branch vs $\hat{\beta}$ for $|\phi_0|=\rho_s/L_n$, $k_y\rho_s=0.25$ (solid line), and $k_y\rho_s=0.5$ (dashed line). (b) Eigenfrequency Ω_0 for drift-Alfvén wave branch vs $\hat{\beta}$ for $|\phi_0|=\rho_s/L_n$, $k_y\rho_s=0.25$ (solid line), and $k_y\rho_s=0.5$ (dashed line).

growth rate for the drift-wave pump and the drift-Alfvén wave pump, respectively, as a function of $\hat{\beta}$ for different $k_x\rho_s$ and $k_y\rho_s=0.25$ are shown.

As seen in Fig. 2(a), for $k_x\rho_s=0.1$ (solid line), the inclusion of finite beta has a stabilizing influence. This stabilization is from all the finite β effects associated with the drift-waves (both the pump and the sidebands). The term associated with the zonal field ψ_s does not contribute to this stablization. For the drift-Alfvén wave pump [Fig. 2(b)], for $k_x\rho_s=0.1$, the growth rate is zero (in the absence of dissipation) (solid line). As $k_x\rho_s$ is increased to 0.25, the drift-wave driven zonal flow growth rate at $\hat{\beta}=0$ increases (dashed line). This is to be expected since the overall growth rate is proportional to $k_x\rho_s$. As beta is increased from zero, the stabilizing influence of the finite beta effects on the drift waves (both pump and side bands) reduces the growth. However beyond a certain $\hat{\beta}$, the growth rate increases. This is due to the zonal field term. If we examine the matrix element M_B which arises from the zonal field term, for instability to occur, $M_B>0$. For the drift wave pump wave, Fig. 1 shows that as $\hat{\beta}$ increases the mode frequency decreases making $M_B>0$. For the drift-Alfvén pump, for $k_x\rho_s=0.25$, the zonal field driven instability occurs for $\hat{\beta}\geqslant 10$. For $k_x\rho_s=0.5$ (long dashed line), in Fig. 2(a), the larger growth rate at $\hat{\beta}=0$ is

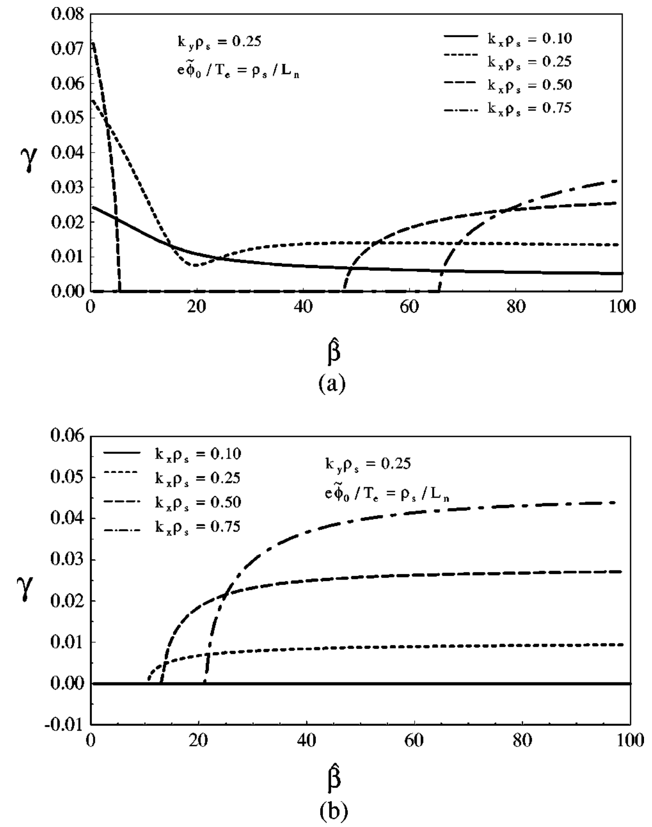

FIG. 2. (a) Growth rate γ for zonal flow/field instability vs $\hat{\beta}$ for drift-wave pump with $|\phi_0|=\rho_s/L_n$ and $k_y\rho_s=0.25$. The different curves are for $k_x\rho_s=0.1$ (solid line), $k_x\rho_s=0.25$ (dashed line), $k_x\rho_s=0.50$ (long dashed line), and $k_x\rho_s=0.75$ (dashed long-dashed line). (b) Growth rate γ for zonal flow/field instability vs $\hat{\beta}$ for drift-Alfvén wave pump with $|\phi_0|=\rho_s/L_n$ and $k_y\rho_s=0.25$. The different curves are for $k_x\rho_s=0.1$ (solid line), $k_x\rho_s=0.25$ (dashed line), $k_x\rho_s=0.50$ (long dashed line), and $k_x\rho_s=0.75$ (dashed long-dashed line).

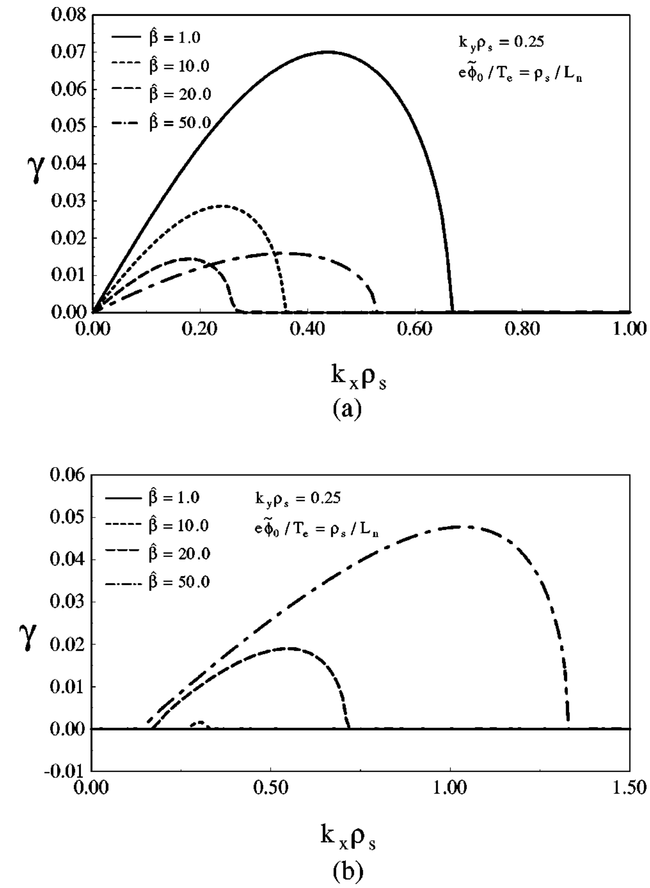

FIG. 3. (a) Growth rate γ for zonal flow/field instability vs $k_x\rho_s$ for drift-wave pump with $|\phi_0|=\rho_s/L_n$ and $k_y\rho_s=0.25$. The different curves are for $\hat{\beta}=1.0$ (solid line), $\hat{\beta}=10.0$ (dashed line), $\hat{\beta}=20.0$ (long dashed line), and $\hat{\beta}=50.0$ (dashed long-dashed line). (b) Growth rate γ for zonal flow/field instability vs $k_x\rho_s$ for drift-Alfvén wave pump with $|\phi_0|=\rho_s/L_n$ and $k_y\rho_s=0.25$. The different curves are for $\hat{\beta}=1.0$ (solid line), $\hat{\beta}=10.0$ (dashed line), $\hat{\beta}=20.0$ (long dashed line), and $\hat{\beta}=50.0$ (dashed long-dashed line).

again due to the increase in $k_x\rho_s$. However the stabilization effect of finite beta together with $\hat{\Delta}$ leads to a stable window in $\hat{\beta}$ space. Finally for large enough $\hat{\beta}$ the destabilizing effect of the zonal field overcomes the threshold and instability prevails. For the drift-Alfvén branch, the onset threshold in $\hat{\beta}$ for $k_x\rho_s=0.5$ is higher compared to the $k_x\rho_s=0.25$ case and the growth rates are higher. This can be understood from the dispersion relation Eq. (17). The threshold in $\hat{\beta}$ can be obtained if we balance the zonal field related term M_B with $\hat{\Delta}^2$. This shows that the value of $\hat{\beta}$ at the threshold should scale as $k_\perp^2$. Also beyond the threshold the growth rate should scale as $k_x\rho_s$ due to the overall linear dependence on this parameter. The curves for $k_x\rho_s=0.75$ (dotted–dashed lines) in Fig. 2(a) and 2(b), support the scalings, with one significant difference. For the drift-Alfvén wave case, the low $\hat{\beta}$ instability has been completely stabilized. The overall conclusion from these plots is that there is a stronger destabilization of the zonal flow and zonal magnetic field for larger $\hat{\beta}$ both for the drift and drift-Alfvén pump waves.

The dependence of the growth rate on $k_x\rho_s$ for different values of $\hat{\beta}$ for the drift-wave pump and the drift-Alfvén wave pump are shown in Figs. 3(a) and 3(b), respectively. For $\hat{\beta}=1.0$, Fig. 3(a) (solid line) shows that the unstable region extends to large $k_x\rho_s$. The cutoff is due to the $\hat{\Delta}$ term. As $\hat{\beta}$ is increased first to 10 (dashed line) and then to 20 (long-dashed line) the instability region shrinks due to the stabilizing influence of β. However, for $\hat{\beta}=50$ (dashed-long dashed line) the destabilizing influence from the zonal field kicks in and the region of instability then increases. For the drift-Alfvén pump [Fig. 3(b)], as we increase $\hat{\beta}$ from 1 to 50, the basic instability domain in $k_x\rho_s$ increases. Again the high k_x cutoff is due to the dispersive term $\hat{\Delta}$.

For the drift-wave pump mode, Figs. 4(a) and 4(b) show the dependence of $k_x\rho_s$ for the maximally growing mode and the maximum growth rate, respectively, as a function of $\hat{\beta}$ for $k_y\rho_s=0.1$ (solid line), $k_y\rho_s=0.25$ (dashed line), and $k_y\rho_s=0.5$ (dashed long-dashed line). For $k_y\rho_s=0.1$, the stablizing influence of finite beta dominates and the mode number for the maximally growing mode decreases. This is true for realistic values of $\hat{\beta}$. For unrealistically larger values of $\hat{\beta}$, the destabilization by coupling to the zonal field finally dominates. However, for the larger $k_y\rho_s$ the destabilizing influence of the zonal field coupling dominates for reasonable

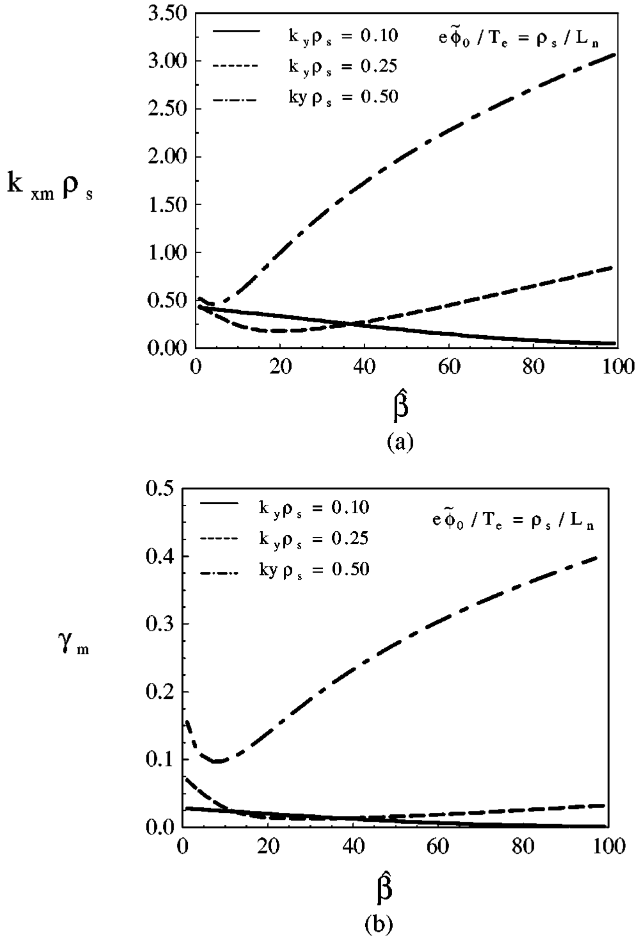

FIG. 4. (a) Wave number with maximum growth rate $k_{xm}\rho_s$ vs $\hat{\beta}$ for drift-wave pump with $|\phi_0|=\rho_s/L_n$ and $k_y\rho_s=0.25$. The different curves are for $k_y\rho_s=0.1$ (solid line), $k_y\rho_s=0.25$ (dashed line), and $k_y\rho_s=0.5$ (dashed long-dashed line). (b) Maximum growth rate γ_m vs $\hat{\beta}$ for drift-wave pump with $|\phi_0|=\rho_s/L_n$ and $k_y\rho_s=0.25$. The different curves are for $k_y\rho_s=0.1$ (solid line), $k_y\rho_s=0.25$ (dashed line), and $k_y\rho_s=0.5$ (dashed long-dashed line).

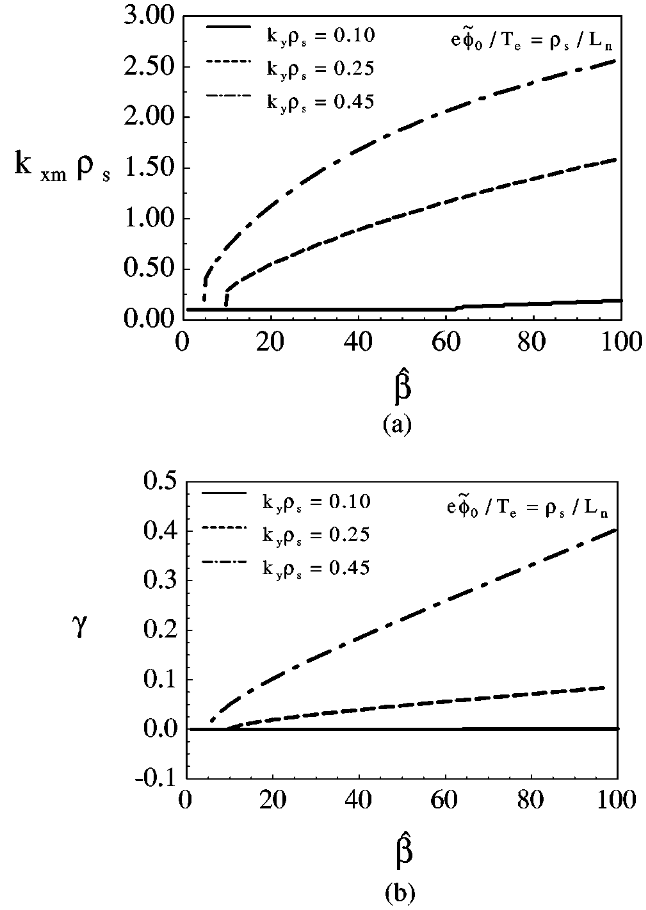

FIG. 5. (a) Wave number with maximum growth rate $k_{xm}\rho_s$ vs $\hat{\beta}$ for drift-Alfvén wave pump with $|\phi_0|=\rho_s/L_n$ and $k_y\rho_s=0.25$. The different curves are for $k_y\rho_s=0.1$ (solid line), $k_y\rho_s=0.25$ (dashed line), and $k_y\rho_s=0.5$ (dashed long-dashed line). (b) Maximum growth rate γ_m vs $\hat{\beta}$ for drift-Alfvén wave pump with $|\phi_0|=\rho_s/L_n$ and $k_y\rho_s=0.25$. The different curves are for $k_y\rho_s=0.1$ (solid line), $k_y\rho_s=0.25$ (dashed line), and $k_y\rho_s=0.5$ (dashed long-dashed line).

but larger $\hat{\beta}$. There is in fact a rapid increase in growth rate as $k_y\rho_s$ increases and the maximally growing mode shifts to higher $k_x\rho_s$. A completely similar trend is also seen for the drift-Alfvén wave pump in Figs. 5(a) and 5(b) which displays the dependence of $k_x\rho_s$ for the maximally growing mode and the maximum growth rate, respectively, as a function of $\hat{\beta}$ for $k_y\rho_s=0.1$ (solid line), $k_y\rho_s=0.25$ (dashed line), and $k_y\rho_s=0.5$ (dashed long-dashed line). Thus by investigating the simple dispersion relation Eq. (17), we find that for finite β plasmas, the generation of zonal flow and fields is markedly different compared to the pure electrostatic case. The coupling to the zonal field allows for a strong destabilization of such flows with the increase of plasma β.

V. CONCLUSIONS

We have derived a dispersion relation for the modulational instability of drift-wave and drift-Alfvén waves in finite β plasmas. The instability analysis involves the coupling of the drift wave (or drift-Alfvén waves) to drift-wave sidebands (or drift-Alfvén wave side bands) and zonal flow as well as zonal fields. For drift-waves and zonal flows/fields with low mode numbers, $k_x\rho_s<0.1$ and $k_y\rho_s<0.1$, the finite beta effect leads to stabilization of the zonal flow/field instability in the parameter region of interest. The dominant finite beta effect in this regime is the finite beta modification of pump and sideband drift waves. On the other hand, for $k_x\rho_s>0.1$ and $k_y\rho_s>0.1$ the increase in finite beta leads to a dramatic increase in the growth rate for the zonal flow/field instability. This high k result also holds for the drift-Alfvén branch. For the low k case, for the drift-Alfvén branch, the zonal flow/field instability is absent. The strong destabilization of the zonal flow/field which increases with β provide a plausible explanation of the transition to H modes by increasing β as seen in the simulations of Rogers *et al.*[30] This issue has been addressed in a recent paper by us.[28] We will will apply the problem of the generation of the shear and zonal flows and fields to the Alfvén waves in the high latitude ionosphere and interplanetary space where shear Alfvén solitons occur in abundance. Also, the present study needs to be extended because of the following limitations. The maximally growing mode shifts to higher $k_x\rho_s$ as $\hat{\beta}$ increases both for the drift wave as well as the drift-Alfvén wave. Thus we need to include finite ion Larmor radius effects, as well as electron inertial effects (which will appear in the magnetic zonal flow). Also, the theory should be extended to the nonlocal case. This will address the issue of the radial structure of zonal flows. For L–H transitions in tokamaks this is an important problem. Finally, a low-dimensional model that describes the nonlinear state of the flows and fields needs to be developed and investigated. All these issues will be addressed in future work.

Note added in proof. After submission of this paper we received a preprint on the same topic. It was recently published [L. Chen, Z. Lin, R. B. White, and F. Zonca, Nucl. Fusion **41**, 747 (2001)].

[1]F. Wagner, G. Becker, K. Behringer, D. Cambell, A. Eberhagen, W. Engelhardt, G. Fussman, O. Gehre, J. Gernhardt, G. V. Gierke, G. Haas, M. Huang, F. Karger, M. Keilhacker, O. Kluber, M. Kornherr, K. Lackner, G. Lisitano, G. G. Lister, H. M. Mayer, D. Meisel, E. R. Muller, H. Murmann, H. Niedermeyer, W. Poschenrieder, H. Rapp, H. Rohr, F. Schneider, G. Siller, E. Speth, A. Stabler, K. H. Steuer, G. Venus, O. Vollmer, and Z. Yu, Phys. Rev. Lett. **49**, 1408 (1982).
[2]K. H. Burrell, T. N. Carlson, E. J. Doyle, D. Finkenthal, P. Gohil, R. J. Groebner, D. L. Hillis, J. Kim, H. Matsumoto, R. A. Moyer, T. H. Osborne, C. L. Rettig, W. A. Peebles, T. L. Rhodes, H. St. John, R. D. Stambaugh, M. R. Wade, and J. G. Watkins, Plasma Phys. Controlled Fusion **34**, 1859 (1992).
[3]R. J. Groebner, Phys. Fluids B **5**, 2343 (1993). This reference provides a comprehensive, chronological survey of the observation of H-modes in major tokamak devices.
[4]F. M. Levinton, M. C. Zarnstorff, S. H. Batha, M. Bell, R. E. Bell, R. V. Bundy, C. Bush, Z. Chang, E. Fredrickson, A. Janos, J. Manickam, A. Ramsey, G. L. Schmidt, E. Synakowski, and G. Taylor, Phys. Rev. Lett. **75**, 4417 (1995).
[5]F. X. Söldner and the Jet Team, Plasma Phys. Controlled Fusion **39B**, 353 (1997).
[6]R. T. Tsunoda, Rev. Geophys. **26**, 719 (1988).
[7]Su. Basu, S. Basu, E. Mackenzie, P. F. Fougere, W. R. Coley, N. C. Maynard, J. D. Winningham, M. Sugiura, W. B. Hanson, and W. R. Hoegy, J. Geophys. Res. **93**, 115 (1988).
[8]G. Ganguli, M. J. Keskinen, H. R. Romero, R. Heelis, T. Moore, and C. Pollock, J. Geophys. Res. **99**, 8873 (1994).
[9]P. Tabeling, P. Perrin, and S. Fauve, Europhys. Lett. **3**, 459 (1987).
[10]O. Cordoso, H. Williame, and P. Tabeling, Phys. Rev. Lett. **65**, 1869 (1990).
[11]P. Tabeling, O. Cardoso, and B. Perrin, J. Fluid Mech. **213**, 511 (1990).
[12]H. Williame, O. Cardoso, and P. Tabeling, Phys. Rev. Lett. **67**, 3247 (1991).
[13]P. N. Guzdar, R. G. Kleva, and L. Chen, Phys. Plasmas **8**, 459 (2001).
[14]L. N. Howard and R. Krishnamurti, J. Fluid Mech. **170**, 385 (1986).
[15]J. Drake, J. Finn, P. Guzdar, V. Shapiro, V. Shevchenko, F. Waelbroeck, A. Hassam, C. S. Liu, and R. Sagdeev, Phys. Fluids B **4**, 488 (1992).
[16]J. M. Finn, J. F. Drake, and P. N. Guzdar, Phys. Fluids B **4**, 2758 (1992).
[17]K. B. Hermiz, P. N. Guzdar, and J. M. Finn, Phys. Rev. E **51**, 325 (1995).
[18]P. N. Guzdar, Phys. Plasmas **2**, 4174 (1995).
[19]L. Chen, Z. Lin, and R. White, Phys. Plasmas **7**, 3129 (2000).
[20]F. Jenko, W. Dorland, M. Kotschenreuther, and B. N. Rogers, Phys. Plasmas **7**, 1904 (2000).
[21]V. B. Lebedev, P. H. Diamond, V. D. Shapiro, and G. I. Soloviev, Phys. Plasmas **2**, 4420 (1995).
[22]P. K. Kaw and R. Singh, Bull. Am. Phys. Soc. **44**, RP01, 109 (1999).
[23]A. I. Smolyakov, P. H. Diamond, and M. Malkov, Phys. Rev. Lett. **84**, 491 (2000).
[24]A. I. Smolyakov, P. H. Diamond, and V. I. Shevchenko, Phys. Plasmas **7**, 1349 (2000).
[25]R. Z. Sagdeev, V. D. Shapiro, and V. I. Shevchenko, Sov. J. Plasma Phys. **4**, 306 (1978).
[26]V. D. Shapiro, P. H. Diamond, V. B. Lebedev, G. I. Soloviev, and V. I. Shevchenko, Plasma Phys. Controlled Fusion **35**, 1033 (1993).
[27]I. Gruzinov, A. Das, P. Diamond, and A. Smolyakov, ''Fast zonal field dynamo in collisionless kinetic Alfvén wave turbulence,'' Phys. Rev. Lett. (submitted).
[28]P. N. Guzdar, R. G. Kleva, A. Das, and P. K. Kaw, Phys. Rev. Lett. **86**, 15 001 (2001).
[29]A. Zeiler, J. F. Drake, and B. Rogers, Phys. Plasmas **4**, 2134 (1997).
[30]B. Rogers, J. F. Drake, and A. Zeiler, Phys. Rev. Lett. **81**, 4396 (1998).